J Mater Sci: Mater Med (2007) 18:705–714
DOI 10.1007/s10856-006-0012-2

The influence of surface chemistry and topography on the contact guidance of MG63 osteoblast cells

F. S. Magdon Ismail · R. Rohanizadeh · S. Atwa · R. S. Mason · A. J. Ruys · P. J. Martin · A. Bendavid

Received: 20 October 2005 / Accepted: 29 December 2005 / Published online: 2 December 2006

Abstract The purpose of the present study was to determine in vitro the effects of different surface topographies and chemistries of commercially pure titanium (cpTi) and diamond-like carbon (DLC) surfaces on osteoblast growth and attachment. Microgrooves (widths of 2, 4, 8 and 10 μm and a depth of 1.5–2 μm) were patterned onto silicon (Si) substrates using microlithography and reactive ion etching. The Si substrates were subsequently vapor coated with either cpTi or DLC coatings. All surfaces were characterized using atomic force microscopy (AFM), scanning electron microscopy (SEM), X-ray photoelectron spectroscopy (XPS) and contact angle measurements. Using the MG63 Osteoblast-Like cell line, we determined cell viability, adhesion, and morphology on different substrates over a 3 day culture period. The results showed cpTi surfaces to be significantly more hydrophilic than DLC for groove sizes larger than 2 μm. Cell contact guidance was observed for all grooved samples in comparison to the unpatterned controls. The cell viability tests indicated a significantly greater cell number for 8 and 10 μm grooves on cpTi surfaces compared to other groove sizes. The cell adhesion study showed that the smaller groove sizes, as well as the unpatterned control groups, displayed better cell adhesion to the substrate.

F. S. M. Ismail (✉) · A. J. Ruys
Biomedical Engineering, School of Aerospace, Mechanical and Mechatronic Engineering, University of Sydney, Sydney, NSW 2006, Australia
e-mail: sism6112@mail.usyd.edu.au

R. Rohanizadeh · S. Atwa · R. S. Mason
Department of Physiology, University of Sydney, Sydney, NSW 2006, Australia

P. J. Martin · A. Bendavid
CSIRO, Industrial Physics, PO Box 218, Lindfield, NSW 2070, Australia

1 Introduction

Understanding the role of surface topography and chemical functionality on growth and adhesion of cells to biomaterials is important in improving tissue/implant interfacial strength. When bone cells are attached on a solid substrate their behavior and function depends on the physico-chemical and morphological properties of the biomaterial surface [1]. These surface characteristics determine how biological molecules will adsorb on the surface and more particularly determine the orientation of adsorbed molecules [2]. Cell-material interaction occurs in two phases, the first phase involves the attachment, adhesion and spreading of the cells and it is the quality of this first phase that influences the second phase, the capacity of the cell to proliferate and differentiate itself on contact with the implant [1]. Early in-vitro cytocompatibility studies focused on the morphological aspect, growth capacity and the state of differentiation of cells on materials with various chemical compositions [3–9]. The diversity of cell responses to the different materials tested highlighted the capacity of cells to discriminate between different surface chemistries [1].

The present study is concentrated on the effect of surface topography on the first phase of bone cell growth and how cpTi and DLC chemistry influences

this process. The surface topographies used in this study were developed by lithographic methods. The transition of lithographic techniques from the semiconductor industry to the field of material science has been a successful and beneficial shift. Many studies have employed lithographic techniques to study cell interactions on a range of topographies [10–12]. A considerable number of these studies were conducted using osteoblast cells on polymer replicas of etched Si wafers and a few coated these polymers with either titanium or titanium alloy coatings. As yet no study, to the knowledge of the authors, has evaluated bone cell growth on DLC coatings on well-structured topographies. This study addresses this issue and provides a direct comparison of results with titanium coated substrata.

Titanium (Ti) is a well-established biomaterial, used successfully in the fabrication of hard-tissue implants, particularly in load bearing applications. However, due to the generally rather biopassive properties of the titanium [13], the healing process is slower compared to other implant materials with bioactive properties (e.g. hydroxyapatite (HA) or HA-coated implants). Research has shown that bone interlocking or micromechanical anchorage at the interface is not a feature common to all surfaces; to achieve it, a certain level of roughness is required [14]. Altering the surface topography of titanium implants has been seen as a method for hastening the bone healing process. At present, titanium implants in clinical use vary with respect to surface roughness and composition, with agreement being limited to the fact that bone forms more readily on rough surfaces whereas fibrous connective tissue is found more frequently on smooth surfaces [15]. In vitro studies have shown that osteoblast-like cells exhibit roughness-dependent phenotypic characteristics [16]. The cells tend to attach more readily to surfaces with a rougher microtopography [16, 17]. Martin et al. and Kieswetter et al. [18, 19] had found that proliferation and differentiation of MG63 cells on titanium surfaces were affected by the surface roughness. Kieswetter et al. [19] more specifically observed that cell proliferation was reduced but not blocked by the surface topography and phenotypic differentiation was enhanced by rougher surface topographies. These tests were conducted on randomly roughened surfaces obtained through coarse grit blasting for moderately rough surfaces and via Ti plasma spraying to prepare very rough surfaces. Much of the research on Ti roughness and its effect on bone cells has been on randomly roughened surfaces [20–22].

Titanium has been a successful implant material due to its biocompatibility, strength and corrosion resistance. It derives its corrosion resistance from the adherent oxide layer, which forms spontaneously at its surface [23]. There is no perceptible degradation except if this layer is disturbed. Titanium does interact with its environment. It has been shown to release metal ions and compounds into the tissues and conversely, oxygen diffuses into it [23, 24]. Conversely, DLC derives its resistance from its amorphous crystal structure, which is not as easily disrupted [25, 26]. DLC is an amorphous, carbon-based film, which possess similar physical properties of crystalline diamond. The molecular structure of these diamond-like carbon (DLC) films is highly variable but all contain a mixture of sp^3 and sp^2 coordinated carbon and significant amounts of hydrogen [25–27]. Although the specific properties of an individual DLC film depend upon the deposition conditions [28–30], generally films are chemically inert and hard, possessing low coefficients of friction [31, 32]. Allen et al. [33] tested macrophage, fibroblast and osteoblast-like cells in vitro on diamond like carbon coatings and found that there was no evidence that DLC coatings, deposited on a variety of substrates, caused cytotoxicity in vitro. They found that cells grown on the coated substrates exhibited normal cellular growth and morphology, proving the biocompatibility of DLC coatings. Many studies have concentrated on the biocompatibility and general surface properties of DLC films and their affect on cells. There is very little knowledge and study on creating defined topographies in DLC and evaluating its effects on bone cells.

In the present study, lithographic techniques were used in combination with thin film coating technology to create well-defined organized groove structures at roughnesses at or below cell dimensions to evaluate MG63 cell performance. This study enabled us to separately evaluate cpTi and DLC film chemistry and topography on osteoblast-like cells and also to directly compare the performance of DLC with that of cpTi.

2 Materials and methods

2.1 Preparation of specimens

Circular silicon discs of 15 mm diameter were cut from 10 cm semiconductor grade single crystal silicon (100) wafers. A pretreatment procedure of ultrasonically cleaning with acetone and then ethanol for 5 min in each was applied to all discs. A few discs with unaltered surface topography were retained as controls. Microlithography was used on all other discs to

create parallel groove patterns with groove and ridge widths of 2, 4, 8 and 10 μm and a depth between 1.5 and 2 μm. All discs were vapor coated with a 300 nm layer of chromium (Cr). A layer of photoresist (Shipley Microposit S1813 photo resist) was applied to the surface of the disc by spin coating. This produced a thin uniform layer of photoresist on the wafer surface. A mask (containing the required groove pattern) was placed over the disc and exposed to UV light (Solitec 3000R, 200W UV) for 13 s. The exposed resist was washed using developer solution (Shipley Microposit MF320 Developer). The disc was then immersed in Cr etching solution to transfer the pattern to the Cr layer. The photoresist layer was washed away using acetone solution. Groove patterns were then etched into the silicon wafer using Reactive Ion Etching (RIE) with CF_4 gas at a pressure of 8 Pa, 50 W for 5 min. All lithographic procedures were conducted in a clean room environment to avoid particle contamination. Table 1 shows different sample groups. Each sample group contained 6 discs.

2.2 Thin film coatings of commercially pure Titanium (cpTi) and Diamond-Like Carbon (DLC)

Commercially pure titanium was coated onto the specimens using a filtered arc deposition process at a substrate bias of -50V to produce a film thickness of approximately 240 nm.

Diamond-Like Carbon was coated onto discs using Plasma Enhanced Chemical Vapor Deposition (PECVD) [34]. The coating process occurred in three stages, Si wafers were initially etched at a floating bias of 600 V and 200 W RF power for 3 min, then an intermediate bonding layer of a-SiC(H) was synthesized from tetramethylsilane (200 W RF power, 650 V bias). Finally, the DLC layer was deposited onto the surface with acetylene as the precursor gas at a partial pressure of 6 Pa at 200 W RF power with a floating bias of 550 V for 5 min (film thickness of 200 nm).

2.3 Surface characterization

Prior to cell culture assays all specimens were characterized using atomic force microscopy (AFM), X-ray photoelectron spectroscopy (XPS), surface profilometry, scanning electron microscopy (SEM), and contact angle measurements. Contact AFM was used to ensure the integrity of the groove structures and to identify any flaws that may exist by using a Thermomicroscopes Autoprobe M5. A surface profilometer (DEKTAK 3030) was used to determine coating thickness. Test samples were used with coatings applied to only a portion of the sample and analyzed by generating a step profile of the uncoated to coated areas. The chemical composition of the surface was investigated with XPS using a SAGE 150 system. Two techniques were used to determine coating coverage within the grooves using SEM (Philips XL30). A focused ion beam (FIB) approach was utilized to remove a thin section of a cpTi sample which could then be imaged at a high tilt angle using SEM [35]. DLC coated samples were fractured and viewed under SEM using backscattered electron (BSE) imaging. The surface energy experiments were carried out on a Ramehart contact angle measurement system (Ramehart, New Jersey, USA) equipped with Ramehart software. We chose to use Deionised (DI) water and Glycerol (Gly) to determine the contact angles of the surface. A 3 μL droplet of DI/Gly was placed onto the surface and photographed using a high resolution camera and transferred to the Ramehart program where the angle between the surface of the substrate and the droplet is measured. This test was repeated 5 times at different locations for both liquids. The contact angle results from both liquids were used to determine the surface energy of the substrate. Tests were conducted at room temperature (23°C) at a relative humidity of 28% (Thermo-Hygro).

Table 1 Sample groups (6 samples in each group)

Coating	Surface topography				
cpTi	2 μm	4 μm	8 μm	10 μm	Control
DLC	2 μm	4 μm	8 μm	10 μm	Control

2.4 Cell culture assays

All specimens were sterilized in 70% ethanol for 30 min and exposed to UV light prior to being introduced into 15 mm diameter multi-well plastic dishes. MG63 Osteoblast-like cells, originally derived from osteosarcoma affected bone were seeded onto the specimens along with DMEM containing calcium, supplemented with 10% fetal bovine serum (FBS). The cells were seeded at a density of 20,000 cells/well for cell morphology studies and 70,000 cells/well for cell number and attachment studies, and incubated at 37°C in a humidified atmosphere of 95% air and 5% carbon dioxide. Cultures were conducted over a 3 day period.

2.4.1 Cell morphology

The cells layers were rinsed with pre-warmed Phosphate Buffered Saline (PBS) solution and fixed using 2% glutaraldehyde in PBS. Cells were kept at room

temperature for 1 h and then stored at 4°C for 24 h. The following day, excess glutaraldehyde solution was removed and cells rinsed once more in PBS before being dehydrated progressively in higher concentrations of ethanol baths (50, 70, 80, 90, 95, and 100%, 10 min in each bath). The samples were dried and gold sputter coated for SEM analysis. A Phillips XL30 SEM was used at high vacuum to analyze the samples.

2.4.2 Cell number

The cells were rinsed with PBS solution and then Trypsinized (with 400 μL of 0.2% of Trypsin) for 9 min at 37°C. Once all cells were detached from the surface, the solution was neutralized with 50 μL of FBS and then stained using 200 μL of Trypan Blue. The solution was flushed several times to suspend cells evenly before pipetting 10 μL into a hemacytometer for cell counting.

2.4.3 Cell adhesion

The cells were once again rinsed with pre-warmed PBS. Ethylene Diamine Tetraacetic Acid (EDTA) at a concentration of 0.2% was pipetted into the wells and placed in the incubator at 37°C for 3 min. The solution was neutralized with Dulbecco's Modified Eagle Medium (DMEM) containing Ca^{2+}. The cells were then stained with Trypan Blue and counted using a hemacytometer. The wells were washed once more with PBS and Trypsinized in order to remove all remaining cells for cell counting. The percentage of detached cells was calculated by dividing the number of cells removed by EDTA over the total number of cells removed by Trypsin. The results were presented as the percentage of attached cells after EDTA treatment. The higher the percentage of attached cells, the higher the cell adhesion.

2.5 Statistical analysis

Statistical significance of results was determined using an ANOVA (One-way Analysis of Variance) test with a Tukey–Kramer Multiple Comparisons Test.

3 Results

3.1 Surface characterization

3.1.1 Atomic force microscopy

AFM images were taken of grooved and ungrooved (control) samples. Scans (20 μm × 20 μm) of the controls were taken before and after thin film coating to determine approximately the roughness of the silicon wafers and to establish the level of roughness added through the coating process.

Table 2 showed that the roughness of the coatings and the silicon wafer were negligible in comparison to the groove sizes. Figure 1 showed scans of the different groove sizes. The 4, 8 and 10 μm grooves were scanned at a range of 50 μm × 50 μm, while the 2 μm grooves were scanned at 20 μm × 20 μm as a higher image resolution was needed. The 2 and 4 μm grooves appear to have rather angled walls and smooth groove surfaces. The 8 and 10 μm grooves appear to have nanometer scale roughness along the groove surface.

3.1.2 X-ray photoelectron spectroscopy

XPS data of DLC films were dominated by the Carbon (C1s) peak with a trace of Oxygen (O1s). The O1s peak at 533 eV is mainly attributed to the absorbed oxygen on the film surface due to air exposure. Titanium films were dominated by the O1s and Titanium (Ti2p) peaks with a trace of C1s. The O1s peak at 530.2 eV is due mainly to the oxide layer that is formed on cpTi surfaces. The relatively high amount of C measured was due to the adsorbed organic molecules always found on oxide films that have been exposed and stored under atmospheric conditions [36]. Both films were free of any surface contamination. Table 3 gives the percent chemical composition (atomic weight percent, at w%) of each atom species in both thin film coatings.

3.1.3 Surface profilometery

Table 4 shows the coating thickness for cpTi and DLC coated samples. There was some variability in thickness related to the uniformity of the deposition process.

3.1.4 Scanning electron microscopy

FIB operates by emitting a beam of positively charged particles which rasters across a specimen, the signal (secondary electrons or secondary ions) reflected back at each point is used to generate an image [35].

Table 2 Coating roughness for ungrooved controls

	Roughness (R_a) (nm)
Si Wafer	2.9
cpTi Coating	4.4
DLC Coating	3.6

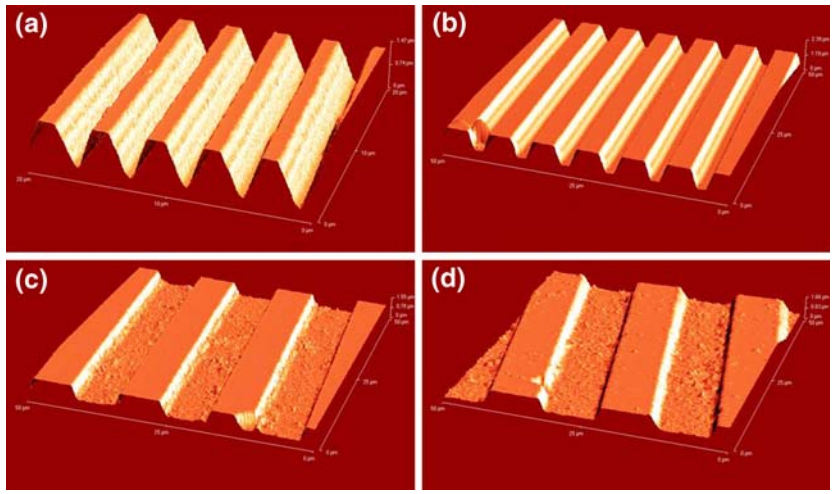

Fig. 1 AFM images of grooved surfaces (**a**) 2 μm (**b**) 4 μm (**c**) 8 μm (**d**)10 μm groove sizes. 2 μm grooves scanned at 20 μm × 20 μm. 4, 8 and 10 μm grooves scanned 50 μm × 50 μm

Table 3 Binding energies and atomic weight percentage of chemical compositions of the coatings materials

		Binding Energy (eV)	Composition (atw %)
cpTi	Ti2p	458.5	16.38
	O1s	530.0	59.15
	C1s	285.0	24.47
DLC	C1s	284.5	97.96
	O1s	533.5	2.04

Table 4 Coating thickness

	Coating Thickness (nm)
CpTi	190–250
DLC	200–260

Sectioned views of cpTi and DLC coated substrates are shown in Fig. 2. Coating penetration was clearly visible in Fig. 2(a) as it is possible to distinguish between the cpTi and Si layers. The highly conductive nature of cpTi resulted in the layer appearing brighter in comparison to the Si substrate. Conversely, the DLC coated sample was indistinguishable from the Si as seen in Fig. 6. Insulating or electrically isolated materials, such as DLC, absorb the particles emitted by the beam and become positively charged upon exposure. Therefore they have a low emission of secondary electrons and appear dark in a secondary image [37]. This combined with a semi conductive Si resulted in an image with little contrast (Fig. 2(b)).

BSE imaging was employed to overcome the non-conductive property of DLC coatings, as it is based on the elemental composition of the material [38]. The efficiency of production of BSE is proportional to the sample material's mean atomic number, which results in image contrast as a function of composition—a higher atomic number material appears brighter than a low atomic number material. Carbon (6) has a lower atomic number than Si (14) and therefore appears darker. Figure 3 showed the darker DLC layer completely coating the Si substrate.

3.1.5 Contact angle measurement

Figure 4 reveals the contact angle results for cpTi and DLC samples using DI and Gly. The 2–8 μm grooves averaged values between 40 and 80°. The 10 μm

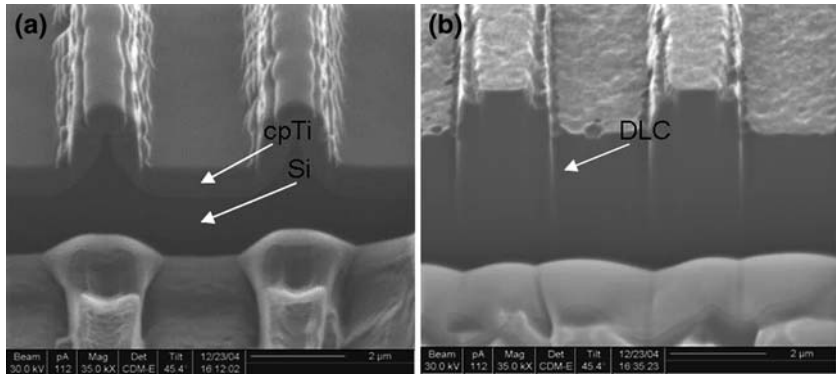

Fig. 2 FIB image of (**a**) cpTi and (**b**) DLC coating layers

samples showed markedly higher contact angles with values greater than 100° especially for DI. The control samples did not show any significant differences between cpTi and DLC and averaged a contact angle of approximately 60°. In general, contact angles <90° are considered hydrophilic and those >90° result in beading on the surfaces and therefore are considered hydrophobic [39]. The 2 μm. cpTi samples for DI and Gly showed significantly greater contact angles compared to the respective controls ($P < 0.001$ for DI and $P < 0.05$ for Gly). The 4 μm cpTi sample for DI showed a significantly lower contact angle compared to its control with a $P < 0.001$. The 10 μm samples for DI showed the largest contact angle with both being significantly greater than its control with $P < 0.001$. The majority of results comparing cpTi to DLC samples did not show any significant differences. The only exceptions were with 2 μm DLC with Gly, 4 μm DLC with DI and 10 μm DLC with Gly (Fig. 4).

Figure 5 shows the surface energy results for cpTi and DLC coated samples. The surface energy results were derived from the contact angles found using DI and Gly with the patterned and control surfaces. Titanium results indicated a significantly greater surface energy for 4 μm grooves compared to the controls with a P-value less than 0.01. Comparing this same sample to the 4 μm DLC, showed that the cpTi sample had a significantly higher surface energy ($P < 0.001$). The 10 μm DLC samples displayed a significantly lower surface energy when compared to DLC control and the 10 μm cpTi sample ($P < 0.001$). The cpTi coated samples averaged a surface energy of about 55 J/m^2. DLC samples exhibited a steady decrease in surface energy from 2 to 10 μm grooves.

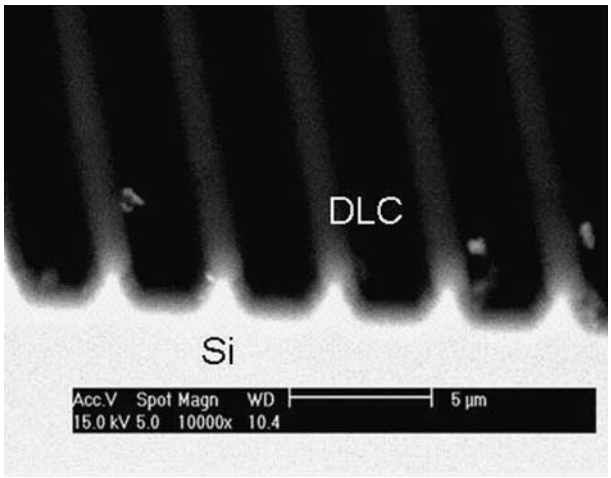

Fig. 3 BSE image of DLC coating

3.2 Cell culture

3.2.1 Cell morphology

Figure 6 shows SEM images of MG63 osteoblast cells cultured on grooved cpTi surfaces. The 2 and 4 μm samples showed the greatest degree of contact guidance (Fig. 6(a) and (b), respectively). The cells on these samples appeared to mainly extend on the ridge surface. Cells grown on the 2 μm surface show a much smaller cell extension. Cell behavior on the 8 and 10 μm samples were quite similar with little contact guidance and a greater cell extension compared to the smaller grooves. For all patterned surfaces with cpTi coatings, cell fibrils were located mainly at the ends of the cell.

Figure 7 shows the morphology of MG63 cells on grooved DLC coated samples. Once again, the 2 and 4 μm samples displayed the greater contact guidance. Cells on these groove sizes appeared much flatter along the ridge surface. Cell extension on the 4 μm grooves were much greater than with the 2 μm samples. The 8 μm grooves produced a much more rounded cell, which was not as well oriented along the parallel grooves. There was a considerably greater cell extension on the 10 μm samples, however contact guidance was not significant.

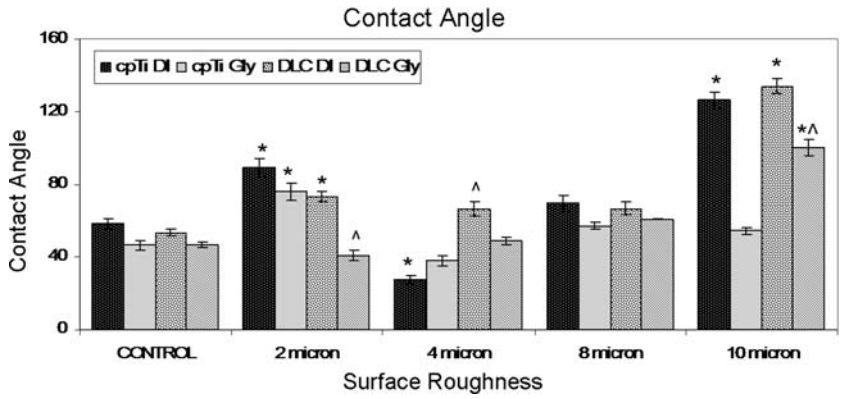

Fig. 4 Contact angle results for cpTi and DLC using DI and Gly as test liquids. Columns marked with the *, represent significant results for cpTi and DLC compared to the respective controls. Columns marked with the ^, represent significant results for DLC in comparison to the respective cpTi results

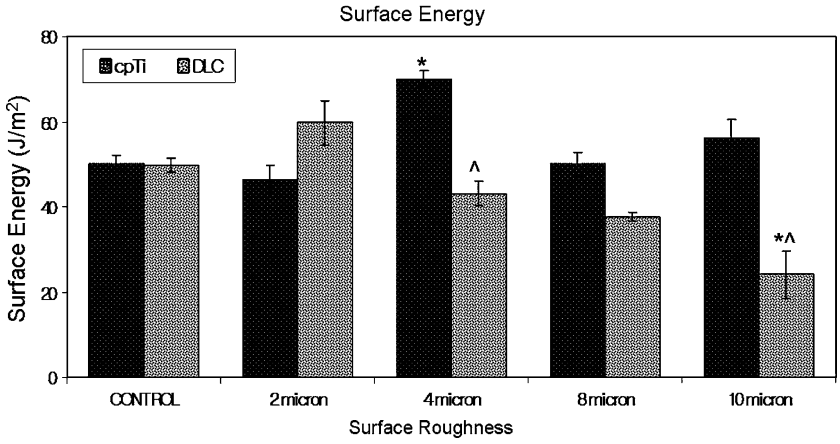

Fig. 5 Surface energy results of DI and Gly. Columns marked with the *, represent significant results for cpTi and DLC compared to the respective controls. Columns marked with the ^, represent significant results for DLC in comparison to the respective cpTi results

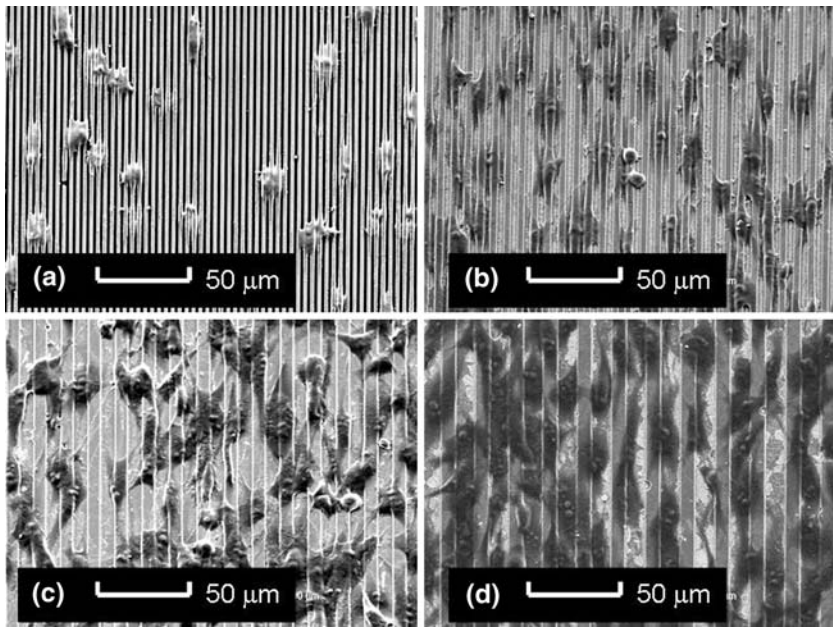

Fig. 6 SEM (×1000) images of MG63 cells on cpTi coated (**a**) 2 μm (**b**) 4 μm (**c**) 8 μm and (**d**) 10 μm grooves

Both control surfaces (Fig. 8) showed the random orientation of cells on unpatterned surfaces. Titanium coated surfaces produced a much flatter morphology with focal adhesions progressing in all directions compared to the DLC control.

In comparison to the controls, which displayed a more disorganized cell layout, all grooved samples appeared to have initiated some degree of contact guidance. The cpTi and DLC coated samples exhibited a similar trend for all groove sizes. The two larger groove sizes displayed cell growth within the grooves and on ridge surfaces with minimal impact on cell guidance. The 8 μm samples showed a more rounded cell shape. The smaller grooves only supported cell growth on the ridges however appeared to influence cell contact guidance a great deal more.

3.2.2 *Cell number*

Figure 9 gives the cell count after a 3 day culture. The cpTi samples showed a general increase in counts with groove size. The 2, 8 and 10 μm samples showed a significantly greater cell count compared to its controls with P values of <0.05, <0.001 and <0.001, respectively. The DLC samples showed little variation between the groove sizes; however the results were comparable to the TCP. Comparing cpTi and DLC, we saw a significantly higher count for 2, 8 and 10 μm cpTi specimens with $P < 0.001$.

3.2.3 *Cell attachment*

Figure 10 displays the level of osteoblast attachment after a 3 day culture period. Statistical results indicated

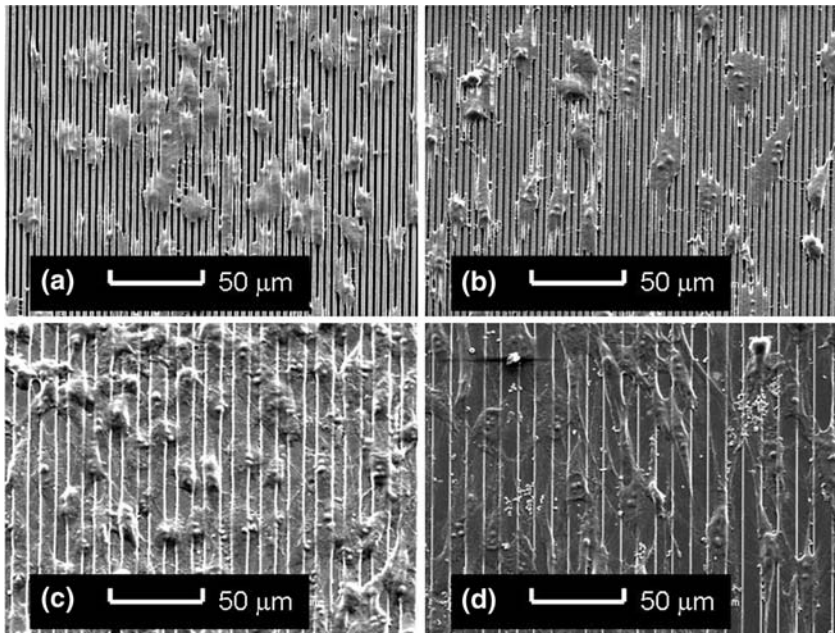

Fig. 7 SEM (×1000) images of MG63 cells on DLC coated (**a**) 2 μm (**b**) 4 μm (**c**) 8 μm and (**d**) 10 μm grooves

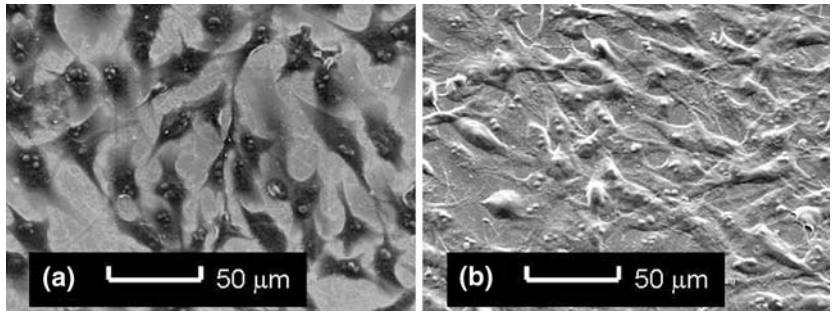

Fig. 8 SEM (×1000) images of MG63 cells on (**a**) cpTi and (**b**) DLC controls

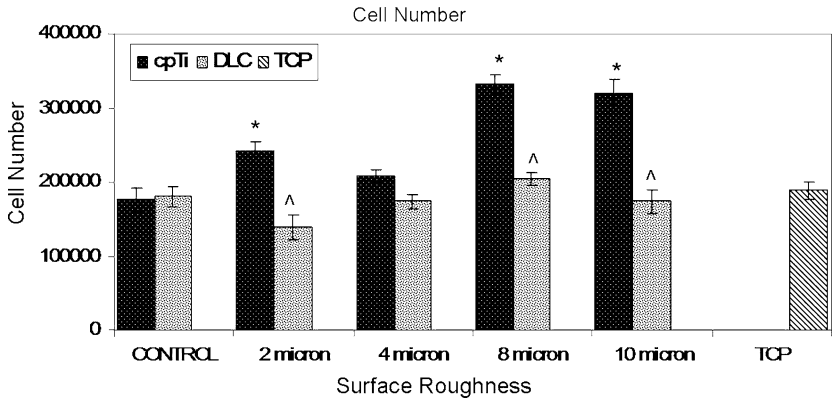

Fig. 9 Cell viability after 3 day culture for cpTi, DLC and tissue culture plastic (TCP). Columns marked with the *, represent significant results for cpTi and DLC compared to the respective controls. Columns marked with the ^, represent significant results for DLC in comparison to the respective cpTi results

no significant differences between cpTi coated samples with an average attachment level of 80%. The level of attachment was slightly lower for 4 μm cpTi samples, however it was not found to be significant. DLC coated samples showed no significant differences for 2, 8 and 10 μm groove sizes compared to the control with about an 80% attachment rate. Only the 4 μm DLC sample showed a significantly lower percentage of attachment ($P < 0.001$) compared to its control, with levels about 50%.

4 Discussion

Interactions between biomaterials and cells mainly depend on surface characteristics of the biomaterial,

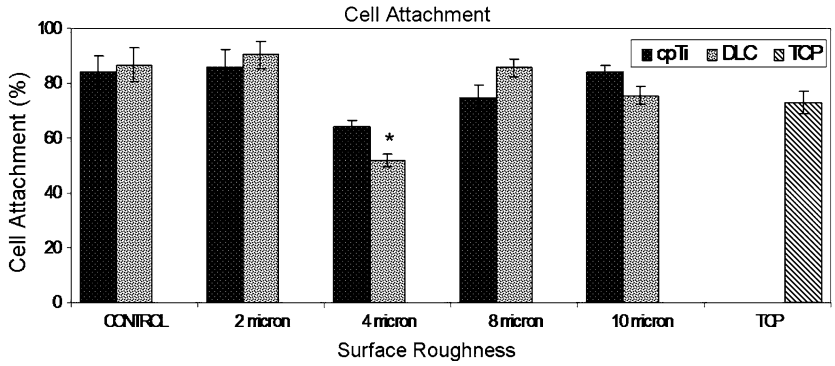

Fig. 10 Cell attachment after 3-day culture. Columns marked with the *, represent significant results for cpTi and DLC compared to the respective controls

including surface topography, chemistry, and charge. This study examined the MG63 osteoblast growth and attachment on cpTi and DLC surfaces with modified surface topographies.

Our research examined the contact angles and surface energies of cpTi and DLC films on patterned and control surfaces. Tests were conducted using DI and Gly. Surfaces are considered hydrophilic if their contact angles are below 90° [39]. Our results indicated that all surfaces with groove size less than 8 μm were hydrophilic as they averaged a contact angle of about 80°. In order to establish how comparable our results were to other studies, we referred to work by Keller et al who reported contact angles of about 52° for cpTi surfaces with a 1 μm surface roughness. This result was comparable to the contact angles obtained on our cpTi control surfaces, which averaged about 58°. The slight variance would be due to differences in humidity levels and the highly polished nature of our specimens. Contact angle results were utilized to calculate the surface energy of the thin films. Surface energy has been found to influence cell behavior with cells being more prone to attach and spread on surfaces with higher surface energies [40, 41]. This was not as apparent from the results obtained, which showed a significantly higher surface energy for 4 μm cpTi, however a slightly lower cell attachment rate in comparison to the results from the other surface types. The 10 μm DLC showed a significantly lower surface energy than that of cpTi however it achieved a similar level of cell attachment. Surface energy levels did not appear to affect the level of cell attachment as much as indicated by other studies.

Morphological evaluation of the cells revealed contact guidance occurring in all grooved samples on both cpTi and DLC. The degree of guidance and alignment was greater along smaller grooves (2 and 4 μm) despite cells bridging the groove structures. The results were similar to a study of osteoblast cells on smooth and microgrooved (groove depth 0.5–1.5 μm, groove and ridge width 1–10 μm) polystyrene substrates. SEM of these cells showed that the cells, and their extensions, closely followed the surface on smooth and wider grooved (>5 μm) substrates, with narrow grooves (<2 μm) being bridged [42]. A comparison of cell morphology between the cpTi and DLC coatings showed that cells appear flatter on cpTi samples for most groove sizes. Higher cell numbers for 2, 8 and 10 μm grooves on cpTi substrates was in accordance with the results published by Hunter et al. [9] who reported that one of the main regulators of proliferative rate in anchorage dependent cells is shape. Cells in a rounded configuration divide at a lower rate than those flattened and well spread on a substratum. Consequently, cells which attach to materials but spread little will show lower proliferative rates than those materials which allow greater spreading [9]. Cell morphology, as well as affecting cell numbers, also affects the degree of cell attachment. Aligned cells are said to demonstrate more favorable adhesion behavior than a spherically shaped cell. This has been attributed to a higher density of focal contacts when they were in contact with the edges of the grooves and showed a better organization of the cytoskeleton and stronger actin fibers [43]. The present results indicated 2, 8 and 10 μm grooves experienced relatively good attachment for cpTi and DLC samples which can be linked to SEM images that indicate contact guidance (cell alignment).

5 Conclusions

- Microlithographic techniques together with well-established coating deposition technique were an effective means of assessing cell growth on desired surface topographies.
- Osteoblast cells did not show any clear preference for a particular groove size or biomaterial surface.

- Grooved surfaces showed contact guidance in comparison to the disorganized cell layout on control surfaces. A greater degree of guidance was seen on 2 and 4 μm grooves.
- Cell number studies indicated significantly greater numbers of osteoblast cells on 2, 8 and 10 μm grooved cpTi coated samples compared to the DLC coated surface.
- Cell attachment levels for 2, 8 and 10 μm grooves were quite good at about 80% for cpTi and DLC samples.
- Overall DLC coatings appeared to have a similar impact on osteoblast-like cells as cpTi.

Acknowledgments The authors would like to warmly thank Dr Z. Xie (Materials Science, University of New South Wales) for assistance with FIB, and Mr. Tony Romeo and Dr Ian Kaplin (Electron Microscopy Unit, University of Sydney) for assistance with electron microscopy.

References

1. K. ANSELME, *Biomat* **21** (2000) 667
2. B. D. BOYAN, T. W. HUMMERT, D. D. DEAN and Z. SCHWARTZ, *Biomat* **17** (1996) 137
3. J. C. KELER, C. M. STANFORD, J. P. WIGHTMAN, R. A. DRAUGHN and R. ZAHARIAS, *J. Biomed. Mater. Res*. **28** (1994) 939
4. U. MEYER, D. H. SZULCZEWSKI, K. MOLLER, H. HEIDE and D. B. JONES, *Cells and Mater*. **3** (1993) 129
5. D. DE SANTIS, C. GUERRIERO, P. F. NOCINI, A. UNGERSBOCK, G. RICHARDS, P. GOTTE and U. ARMATO, *J. Mater. Sci. Mater in Med*. **7** (1996) 21
6. N. ABDESSAMAD and M. F. HATMAND *J. Biomed. Mater. Res*. **24** (1990) 861
7. C. R. HOWLETT, M. D. M. EVANS, W. R. WALSH, J. GRAHAM and J. G. STEELE, *Biomat*. **15** (1994) 213
8. D. A. PULEO and R. BIZIOS *J. Biomed. Mater. Res*. **26** (1992) 291
9. A. HUNTER, C. W. ARCHER, P. S. WALKER and G. W. BLUNN, *Biomat*. **16** (1995) 287
10. P. CLARK, G. A. DUNN, A. KNIBBS and M. PECKHAM, *Int. J. Biochem. Cell Biol,*. 34 (2002) 816
11. A. I. TEIXEIRA, G. A. ABRAMS, C. J. MURPHY and P. F. NEALEY *J. Vac. Sci. & Technol.* B **21** (2003) 683
12. S. LENHERT, M. B. MEIER, U. MEYER, L. CHI and H. P. WIESMANN *Biomat.* **26** (2005) 563
13. S. G. STEINEMANN , Periodont. 2000, **17** (1998) 7
14. S. SZMUKLER-MONCLER, D. PERRIN, V. AHOSSI, G. MAGNIN and J. P. BERNARD, *J. Biomed. Mater. Res*. **68B** (2004) 149
15. D. L. COCHRAN, J. SIMPSON, H. WEBER and D. BUSER, *Int. J. Oral Maxillo. Imp*. **9** (1994) 289
16. K. T. BOWERS, J. C. KELLER, B. A. RANDOLPH, D. G. WICK and C. M. MICHAELS, *Int. J. Oral Maxillo. Imp*. **7** (1992) 302
17. C. M. MICHAELS, J. C. KELLER, C. M. STANFORD and M. SOLURSH, *J. Dent. Res*. **68** (1989) 276
18. J. Y. MARTIN, Z. SCHWARTZ, W. HUMMERT, D. M. SCHRAUB, J. SIMPSON, J. LANKFORD JR, D. D. DEAN, D. L. COCHRAN and B. D. BOYAN, *J. Biomed. Mater. Res*. **29** (1995) 389
19. K. KIESWETTER, Z. SCHWARTZ, T. W. HUMMERT, D. L. COCHRAN, J. SIMPSON, D. D. DEAN and B. D. BOYAN, *J. Biomed. Mater. Res*. A **32** (1996) 55
20. J. LINCKS, B. D. BOYAN, C. R. BLANCHARD, C. H. LOHMANN, Y. LIU, D. L. COCHRAN, D. D. DEAN and Z. SCHWARTZ, *Biomat*. **19** (1998) 2219
21. D. D. DELIGIANNI, N. KATSALA, S. LADAS, D. SOTIROPOULOU, J. AMEDEE and Y. F. MISSIRLIS, *Biomat*. **22** (2001) 1241
22. M. BIGERELLE, K. ANSELME, B. NOËL, I. RUDERMAN, P. HARDOUIN and A. IOST, *Biomat*. **23** (2002) 1563
23. P. DUCHEYNE, G. WILLEMS, M. MARTENS and J. HELSEN, *J. Biomed. Mater. Res*. **18** (1984) 293
24. J. L. WOODMAN, J. J. JACOBS, J. O. GALANTE and R. M. URBAN, *J. Ortho. Res*. **1** (1984)421
25. S. AISENBERG and R. CHABOT, *J. App. Phys*. **42** (1971) 2953
26. H. C. TSAI and D. B. BOGY, *J. Vac. Sci. Technol*. **A5** (1987) 3287
27. F. JANSEN, M. MACHONKIN, S. KAPLAN and S. HARK, *J. Vac. Sci. Technol*. **A3** (1985) 605
28. J. C. ANGUS and F. JANSEN, *J. Vac. Sci. & Technol*. **A6** (1988) 1778
29. D. R. MCKENZIE, R. C. MCPHEDRAN, N. SAVVIDES and L. C. BOTTER, *Philos. Mag*. **48** (1983) 341
30. C. V. DESHPANDEY and R. F. BUNSHAH, *J. Vac. Sci. & Technol*. **A7** (1989) 2294
31. A. MATTHEWS and S. S. ESKILDEN, *Diam. Films*. **13** (1993) 1
32. A. ERDEMIR, M. SWITALA, R. WEI and P. WILBUR, *Surf. Coat. Technol*. **50** (1991) 17
33. M. ALLEN, F. LAW and N. RUSHTON, *Clin. Mater*. **17** (1994) 1
34. J. JANG , J. H. MOON, E. J. HAN and S. J. CHUNG, *Thin Solid Films*, 341 (1999)
35. M. W. PHANEUF, *Micron*. **30** (1999) 277
36. M. WIELAND, B. CHEHROUDI, M. TEXTOR and D. M. BRUNETTE, *J. Biomed. Mater. Res*. **60** (2002) 434
37. T. K. OLSON , R. G. LEE and J. C. MORGAN, in "18th International Symposium for Testing and Failure Analysis (ISTFA 92)" (Materials Park, Ohio: ASM International, 1992)
38. B. L. GABRIEL, *SEM: A User's Manual For Materials Science* (Metals Park, Ohio 44073: American Society for Metals, 1985)
39. General Electric Company G.E. in http://www.gewater.com/library/tp/772_Hydrophilicity_and.jsp, 1997–2005
40. S. A. REDEY, S. RAZZOUK, C. REY, D. BERNACHE-ASSOLLANT, G. LEROY, M. NARDIN and G. COURNOT, *J. Biomed. Mater. Res*. **45** (1999) 140
41. T. G. VAN KOOTEN, J. M. SCHAKENRAAD, H. C. VAN DER MEI and H. J. BUSSCHER, *Biomat.* **13** (1992) 897
42. K. MATSUZAKA, X. F. WALBOOMERS, M. YOSHINARI, T. INOUE and J. A. JANSEN, *Biomat*. **24** (2003) 2711
43. E. EISENBARTH, P. LINEZ, V. BIEHL, D. VELTEN, J. BREME and H. F. HILDEBRAND, *Biomol. Eng*. **19** (2002) 233